PERGAMON

International Journal of Solids and Structures 37 (2000) 461–475

INTERNATIONAL JOURNAL OF SOLIDS and STRUCTURES

www.elsevier.com/locate/ijsolstr

Crack propagation in heterogeneous media

A.A. Al-Falou*, R.C. Ball

Department of Physics, University of Warwick, Coventry CV4 7AL, UK

Received 6 August 1998; in revised form 4 December 1998

Abstract

We assume that an infinite material contains a point inhomogeneity which has slightly different elastic constants from the rest of the otherwise isotropic and homogeneous elastic material. We evaluate the path of a three-dimensional semi-infinite quasi static crack propagating near this point inhomogeneity. The real space crack path is evaluated as well as the power spectrum of the crack surface. The latter enables us to calculate the roughness exponent for quasi-static fracture. It is also shown how the real space crack surface and its power spectrum can be obtained for an arbitrary distribution of inhomogeneities.

Keywords: Fracture; Inhomogeneity; Roughness exponent; Quasi-static three-dimensional crack propagation

1. Introduction

Most theoretical treatments of crack propagation are based on the assumption that the linear elastic material is isotropic and homogeneous; see for example Lawn (1993), Sih (1973) and Freund (1993). Real materials contain inclusions and, in spite of their practical importance, little is known theoretically about crack propagation in the presence of heterogeneities. The main obstacle to a theoretical analysis of crack propagation in heterogeneous media has been the fact that as a crack passes by an inhomogeneity, it also changes its surface geometry. In turn, this geometrical perturbation influences the direction of crack propagation. Only recently has the relationship between a small perturbation of the crack surface and the direction of crack propagation been quantified in three dimensions (see Ball and Larralde, 1995; Al-Falou et al., 1998). Previous calculations (e.g. Gao, 1992; Xu et al., 1994) lead to similar results apart from a different prefactor of K_{II}. Using this result, we can decompose the calculation of the crack path into the known geometrical contribution and an inhomogeneity contribution which remains to be evaluated in this paper.

The base problem we consider is that of a crack propagating past a point inclusion of (slightly)

* Corresponding author.
E-mail address: phseq@csv.warwick.ac.uk (A.A. Al-Falou)

0020-7683/00/$ - see front matter
PII: S0020-7683(99)00016-5

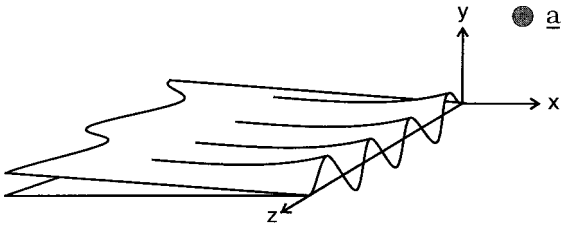

Fig. 1. Crack propagation near a point inhomogeneity at position $\underline{a}$.

different elastic constants from the surrounding medium. We calculate the resulting crack surface deflection to leading, linear order in the elastic constant variation. The linearity of this calculation means that it can be interpreted as the general response function to elastic perturbations, and the response to general (but weak) perturbations is obtained by superposition. For tractability, our calculations are limited to quasi-static type I crack propagation through a locally linear and elastically isotropic material. Restricting the inhomogeneities to isotropic elasticity still leaves the variation of the two Lamé parameters to consider.

The main burden of our calculation is to evaluate the first order mode II stress intensity factor K_{II} (the zeroth order vanishes as the unperturbed crack is purely under mode I loading) along the perturbed crack crack edge. Then the maximal Hoop stress criterion, i.e. $K_{\mathrm{II}}[h]=0$, implies a functional equation for the crack surface $h(x,z)$ determining the path of the crack edge. Here and in the following, the coordinates x, y and z denote the frame of reference of the unperturbed (planar) crack oriented as in Fig. 1.

2. The virtual force from a point inclusion

We anticipate that, in the presence of an inhomogeneity, the geometry of the crack will be slightly disturbed. We can decompose the first order contribution to the displacement field into a geometrical part for the homogeneous material (as if the crack surface were perturbed and the material homogeneous), $\underline{u}_g$, and an inhomogeneous part for a planar crack (as if the crack were planar and the material has an inhomogeneity), $\underline{u}_i$. The total displacement up to first order is

$$\underline{u} = \underline{u}_0 + \underline{u}_g + \underline{u}_i, \tag{1}$$

where $\underline{u}_0$ is the mode I displacement field of the unperturbed crack. Finally, we want to obtain the mode II stress intensity factors $K_{\mathrm{II},g}$ and $K_{\mathrm{II},i}$ associated with $\underline{u}_g$ and $\underline{u}_i$. Note that the stress intensity factor for the geometrical contribution has already been calculated by Ball and Larralde (1995) (see also Al-Falou et al., 1998) to be

$$K_{\mathrm{II},g}(k_z) = \frac{K_{\mathrm{I}}}{2}\left(\frac{\partial h_{k_z}(\ell_x)}{\partial \ell_x} + \frac{2-3\nu}{2-\nu}|k_z| h_{k_z}(\ell_x)\right), \tag{2}$$

where ℓ_x denotes the x position of the crack edge, $h_{k_z}(x)$ is the Fourier transformed vertical perturbation of the planar crack and and $K_{\mathrm{II},g}(k_z)$ is the corresponding transformed mode II stress intensity factor along the crack edge.

In the following, we shall calculate $K_{\mathrm{II},i}$ associated with $\underline{u}_i$. We assume that the material without the inclusion is isotropic and homogeneous with an elastic moduli tensor $\mathbf{C}$, given by

$$C_{ijkl} = \lambda\delta_{ij}\delta_{kl} + \mu(\delta_{ik}\delta_{jl} + \delta_{il}\delta_{jk}). \tag{3}$$

The elastic moduli tensor of the inclusion at the point $\underline{a}$ is $\mathbf{C} + \delta\mathbf{C}f(\underline{x}-\underline{a})$, where we treat $\delta\mathbf{C}$ as a perturbation to first order. To calculate the linear response in the mode II stress intensity factor to a variation of λ, we set $f(\underline{x}-\underline{a}) = \delta V\delta(\underline{x}-\underline{a})$, where δV is the (infinitesimal) volume of the inclusion. The linear equations of elasticity read as:

$$-\nabla\cdot\underline{\underline{\sigma}} = 0$$

with

$$\underline{\underline{\sigma}} = (\mathbf{C} + \delta\mathbf{C}\delta V\ \delta(\underline{x}-\underline{a})):\nabla\underline{u}, \tag{4}$$

and the boundary conditions,

$$\underline{n}\cdot\underline{\underline{\sigma}} = 0 \tag{5}$$

on the planar crack surface, whose outward normal is $\underline{n}$. Inserting $\underline{u} = \underline{u}_0 + \underline{u}_i$ in Eq. (4), we obtain

$$-\nabla\cdot\delta\mathbf{C}\delta V\ \delta(\underline{x}-\underline{a}):\nabla\underline{u}_0 - \nabla\cdot(\mathbf{C} + \delta\mathbf{C}\delta V\ \delta(\underline{x}-\underline{a})):\nabla\underline{u}_i = 0, \tag{6}$$

since, by definition, $\underline{u}_0$ satisfies the linear elastic equations for the elastic moduli tensor $\mathbf{C}$. The boundary conditions become

$$\underline{n}\cdot\delta\mathbf{C}\delta V\ \delta(\underline{x}-\underline{a}):\nabla\underline{u}_0 + \underline{n}\cdot(\mathbf{C} + \delta\mathbf{C}\delta V\ \delta(\underline{x}-\underline{a})):\nabla\underline{u}_i = 0 \tag{7}$$

on the planar crack surface. Neglecting second and higher order contributions in Eqs. (6) and (7), we obtain

$$-\nabla\cdot\mathbf{C}:\nabla\underline{u}_i = \underline{f}_{\text{virtual}}$$

with

$$\underline{f}_{\text{virtual}} = \nabla\delta\mathbf{C}\delta V\ \delta(\underline{x}-\underline{a}):\nabla\underline{u}_0 \tag{8}$$

and

$$\underline{n}\cdot\mathbf{C}:\nabla\underline{u}_i = 0 \text{ on the crack surface.} \tag{9}$$

Note that in the last equation, we have used the fact that the symmetric strain tensor $(\nabla\underline{u}_0)_s$ of a quasi static crack under mode I loading vanishes on the crack surface (see also Ball and Larralde, 1995).

3. K_{II} for a point inclusion

Eqs. (8) and (9) together reduce the problem of a point inclusion to an equivalent force on a planar crack. Using the 3-D mode II weight function $\underline{\mathscr{G}}_{\text{II}}$, given in Appendix A, we now proceed to evaluate the corresponding mode II stress intensity factor. Direct application gives

$$K_{\text{II},i}(Z) = \int_\Omega \mathrm{d}^3x\,\underline{\mathscr{G}}_{\text{II}}(\underline{x},Z)\nabla\delta\mathbf{C}\delta V\ \delta(\underline{x}-\underline{a}):\nabla\underline{u}_0(\underline{x}),$$

$$K_{\text{II},i}(Z) = -\nabla\underline{\mathscr{G}}_{\text{II}}(a_x,a_y,a_z - Z):\delta\mathbf{C}\delta V:\nabla\underline{u}_0(a_x,a_y), \tag{10}$$

where we have integrated by parts to obtain the second equation. We have no contributions from boundary terms since we assume that the inclusion is located in the bulk, that is $a_y \neq 0$, so that the delta function yields zero on the crack faces. With $\delta C_{ijkl} = \delta\lambda\delta_{ij}\delta_{kl} + \delta\mu(\delta_{ik}\delta_{jl} + \delta_{il}\delta_{jk})$, the tensor product in Eq. (10) reads

$$K_{\mathrm{II},i}(Z) = -\delta V[\delta\lambda \operatorname{div} \underline{\mathscr{G}}_{\mathrm{II}} \operatorname{div} \underline{u}_0 + \delta\mu\partial_j\mathscr{G}_i(\partial_i u_{0,j} + \partial_j u_{0,i})]. \tag{11}$$

Note that the three-dimensional weight function as given in Appendix A is still Fourier transformed in its z coordinate. Therefore, we shall calculate the mode II stress intensity factor for each Fourier component $K_{\mathrm{II},i}(\underline{a},k_z)$ and the real space stress intensity factor is obtained from

$$K_{\mathrm{II},i}(\underline{a},Z) = \int_{-\infty}^{\infty} \mathrm{d}k_z K_{\mathrm{II},i}(\underline{a},k_z)\mathrm{e}^{ik_z Z}, \tag{12}$$

where Eq. (11) yields

$$\begin{aligned} K_{\mathrm{II},i}(\underline{a},k_z) = -\delta V\Big[&\delta\lambda \operatorname{div}\Big(\underline{\mathscr{G}}_{\mathrm{II}}(a_x,a_y,-k_z)\mathrm{e}^{-ik_z a_z}\Big) \operatorname{div} \underline{u}_0 \\ &+ \delta\mu\partial_j\Big(\mathscr{G}_i(a_x,a_y,-k_z)\mathrm{e}^{-ik_z a_z}\Big)\big(\partial_i u_{0,j} + \partial_j u_{0,i}\big)\Big]. \end{aligned} \tag{13}$$

Note that derivatives are taken with respect to the $\underline{a}$ coordinates and $\underline{\mathscr{G}}_{\mathrm{II}}(\underline{k})$ and $\underline{u}_0$ are known functions. Since $\operatorname{div} \underline{\mathscr{G}}_{\mathrm{II}}$ and $\operatorname{div} \underline{u}_0$ satisfy Laplace's equation, they have a comparatively simple form, whereas the remainder in Eq. (13) contains the complementary error function. For simplicity of exposition, we shall restrict ourselves to the case where $\delta\mu = 0$ in what follows, thereby avoiding integrals involving the complementary error function. From Lawn (1993), we have

$$\operatorname{div} \underline{u}_0(\underline{x}) = \sqrt{|k_z|}\frac{K_{\mathrm{I}}}{\mu}\frac{(1-2\nu)}{\sqrt{2\pi|k_z|r}}\cos\frac{\phi}{2} \tag{14}$$

and from Appendix A,

$$\begin{aligned} \operatorname{div}\Big(\underline{\mathscr{G}}_{\mathrm{II}}(a_x,a_y,-k_z)\mathrm{e}^{-ik_z a_z}\Big) = &-\sqrt{|k_z|}\,|k_z|\frac{1-2\nu}{2(1-\nu)}\,\frac{1}{\sqrt{2\pi}(|k_z|r)^{3/2}} \\ &\times \mathrm{e}^{-|k_z|r}\left(1 + \frac{2\nu}{2-\nu}|k_z|r + 2\cos\phi + 2|k_z|r\cos\phi\right)\mathrm{e}^{-ik_z a_z}. \end{aligned} \tag{15}$$

Setting these in Eq. (13) with $r = \sqrt{a_x^2 + a_y^2}$, $a_x = r\cos\phi$ and $a_y = r\sin\phi$, we obtain

$$K_{\mathrm{II},i}(\underline{a},k_z) = K_{\mathrm{I}}\frac{\delta V\delta\lambda}{\mu}\frac{(1-2\nu)^2}{8\pi(1-\nu)}a_y|k_z|^3\mathrm{e}^{-|k_z|r}\left(\frac{1}{(|k_z|r)^3} + \frac{2\nu}{2-\nu}\frac{1}{(|k_z|r)^2} + \frac{2|k_z|a_x}{(|k_z|r)^3} + \frac{2|k_z|a_x}{(|k_z|r)^4}\right)\mathrm{e}^{-ik_z a_z}, \tag{16}$$

if the crack tip is at $x = 0$ and the point inclusion at (a_x,a_y,a_z). For an advancing crack whose tip is at $x = \ell_x$, we replace a_x by $a_x - \ell_x$ in the last equation. For a general spatial distribution of inclusions $\delta\lambda(\underline{x})$, we obtain the resulting mode II stress intensity factor from

$$K_{\mathrm{II},i}(k_z) = \int_{\Omega} \mathrm{d}^3 a\,\delta\lambda(\underline{a})K_{\mathrm{II},i}(\underline{a},k_z), \tag{17}$$

where $\delta\lambda$ is replaced by $\delta\lambda(\underline{a})$ in Eq. (16). In the general case, we need to include the response to $\delta\mu \neq 0$

and $\lambda = 0$, which we add to Eq. (16). It is straightforward but cumbersome to compute this expression from Eq. (13).

Physically the restricted case $\delta\mu \approx 0$ can be attained in a material containing a small volume fraction ϕ of voids but otherwise nearly incompressible. This gives

$$\frac{1}{\lambda} = \frac{1}{\lambda_0} + A\frac{\phi}{\mu_0},\ \mu = \mu_0(1 - B\phi), \tag{18}$$

where A and B are positive constants of order unity and the Lamé constants, $\lambda_0 \gg \mu_0$, refer to the voidless case. Then

$$\frac{\delta\lambda}{\lambda} = \frac{-A\delta\phi}{\frac{\mu_0}{\lambda_0} + A\phi} \tag{19}$$

can be large compared to $\delta\mu/\mu = -B\delta\phi$.

4. The evolution equation for the crack tip

We assume that the crack propagates due to the maximal Hoop stress criterion, i.e., in the direction where the total mode II singular stress is zero. We have two contributions to the total mode II stress intensity factor. First, $K_{\mathrm{II},i}$ which arises from the inclusion and which we have calculated above. Second, $K_{\mathrm{II},g}$ from the geometric perturbation of the crack surface from planarity which has been calculated by Ball and Larralde (1995) (see also Al-Falou et al., 1998) is given in Eq. (2). Then the evolution equation is

$$0 = K_{\mathrm{II},g} + K_{\mathrm{II},i}. \tag{20}$$

Substituting Eq. (16) into Eq. (20), the evolution equation becomes

$$\begin{aligned}\frac{\partial h_{k_z}(\ell_x)}{\partial \ell_x} + \frac{2-3\nu}{2-\nu}|k_z|h_{k_z}(\ell_x) = -\delta V\frac{\delta\lambda}{\lambda}\frac{\nu(1-2\nu)}{2\pi(1-\nu)}a_y|k_z|^3 \mathrm{e}^{-ik_z a_z}\mathrm{e}^{-|k_z|r} \\ \times\left(\frac{1}{(|k_z|r)^3} + \frac{2\nu}{2-\nu}\frac{1}{(|k_z|r)^2} + \frac{2|k_z|(a_x-\ell_x)}{(|k_z|r)^3} + \frac{2|k_z|(a_x-\ell_x)}{(|k_z|r)^4}\right),\end{aligned} \tag{21}$$

where $r = \sqrt{(a_x - \ell_x)^2 + a_y^2}$. Note that we have used the relationship $\lambda = \frac{2\nu}{1-2\nu}\mu$.

5. Relating the power spectrum of the crack surface to the distribution of the inhomogeneities

In practice, the power spectrum of the crack surface, $\frac{|\hat{h}(k_x,k_z)|^2}{A_{\|}}$, is measured in diffraction experiments. Here $A_{\|}$ denotes the crack surface area covered by the scattering beam and the reason for dividing by $A_{\|}$ is to define the power spectrum independently of the size of the sample or the scattering beam. In this section we want to relate the power spectrum to the distribution of $\delta\lambda(\underline{a})$. First, we rewrite Eq. (21) for a general distribution $\delta\lambda(\underline{a})$,

$$\frac{\partial h_{k_z}(\ell_x)}{\partial \ell_x} + \frac{2-3\nu}{2-\nu}|k_z|h_{k_z}(\ell_x) = -\frac{\nu(1-2\nu)}{2\pi(1-\nu)\lambda}\int_\Omega \mathrm{d}^3 a\,\delta\lambda(\underline{a})\mathrm{e}^{-ik_z a_z}\hat{g}(\ell_x - a_x, -a_y, k_z), \tag{22}$$

with

$$\hat{g}(x,y,k_z) = -|k_z|^3 y \mathrm{e}^{-|k_z|r}\left(\frac{1}{(|k_z|r)^3} + \frac{2\nu}{2-\nu}\frac{1}{(|k_z|r)^2} - \frac{2|k_z|x}{(|k_z|r)^3} - \frac{2|k_z|x}{(|k_z|r)^4}\right), \tag{23}$$

where $r = \sqrt{x^2+y^2}$ and Ω is the region occupied by the elastic material. We note that the integral on the right hand side of Eq. (22) is a convolution integral with respect to ℓ_x and the Fourier transform of $\delta\lambda(\underline{a})$ with respect to a_z. We now need to Fourier transform $\hat{g}(x,y,k_z)$ in Eq. (23) with respect to x and y to obtain an equation for $\hat{h}(k_x,k_z)$ which relates the experimental data about the power spectrum of the crack surface to the Fourier transformed distribution of inhomogeneities in the bulk of the material. The evaluation of the Fourier transform is straightforward and important steps are given in Appendix B. The final result reads:

$$\hat{h}(k_x,k_z) = -\frac{\nu(1-2\nu)}{(2\pi)^2(1-\nu)\lambda}\frac{\int_{-\infty}^{\infty}\mathrm{d}k_y\hat{g}(\underline{k})\delta\hat{\lambda}(\underline{k})}{ik_x + \dfrac{2-3\nu}{2-\nu}|k_z|}, \tag{24}$$

where the function $\hat{g}(\underline{k})$ is given in Eq. (B4) in Appendix B,

$$\begin{aligned}\hat{g}(\underline{k}) = {} & 2\pi\frac{k_xk_yk_z^2}{\left(k_x^2+k_y^2\right)^2}\left(2 - \frac{k_x^2+k_y^2}{k_z^2} - \frac{2|k_z|}{\sqrt{k_x^2+k_y^2+k_z^2}}\right) \\ & + 2\pi ik_y\left(\frac{1}{\sqrt{k_x^2+k_y^2+k_z^2}} - \frac{2-3\nu}{2-\nu}\frac{k_z^2}{k_x^2+k_y^2}\left(\frac{1}{|k_z|} - \frac{1}{\sqrt{k_x^2+k_y^2+k_z^2}}\right)\right).\end{aligned} \tag{25}$$

Eqs. (24) and (25) constitute the formal linear response of the crack displacement to elastic modulus fluctuations. From these, we can obtain the power spectrum in terms of the distribution $\delta\lambda(\underline{x})$,

$$\frac{|\hat{h}(k_x,k_z)|^2}{A_\parallel} = \frac{1}{A_\parallel}\left(\frac{\nu(1-2\nu)}{(2\pi)^2(1-\nu)\lambda}\right)^2\frac{\int_{-\infty}^{\infty}\mathrm{d}k_y\int_{-\infty}^{\infty}\mathrm{d}k_y'\hat{g}(\underline{k})\delta\hat{\lambda}(\underline{k})\hat{g}(-\underline{k}')\delta\hat{\lambda}(-\underline{k}')}{\left|ik_x + \dfrac{2-3\nu}{2-\nu}|k_z|\right|^2}, \tag{26}$$

where $\underline{k} = (k_x,k_y,k_z)$ and $\underline{k}' = (k_x,k_y',k_z)$.

However, under further assumptions we can relate the spectrum $|\delta\hat{\lambda}(\underline{k})|^2$ directly to the spectrum $|\hat{h}(k_x,k_z)|^2$. Let us assume that we average $|\hat{h}(k_x,k_z)|^2$ over a large number of experiments and that the distribution of inhomogeneities remains the same. In each experiment, the location of the crack surface is arbitrary shifted by an amount $\bar{y}$ with respect to a reference surface. The average over $\bar{y}$ yields zero for the off-diagonal elements of the operator in Eq. (26) since the average over $\bar{y}$ of both sides in Eq. (26) can be written as

$$\langle|\hat{h}(k_x,k_z)|^2\rangle = \int\frac{d\bar{y}}{L_y}\int\mathrm{d}y\int\mathrm{d}y'\int\frac{dk_y}{2\pi}\int\frac{dk_y'}{2\pi}\mathrm{e}^{-ik_yy}\mathrm{e}^{ik_y'y'}f(y-\bar{y})f(y'-\bar{y}), \tag{27}$$

where the integrand in Eq. (26) is abbreviated by $\hat{f}(k_y)\hat{f}(k_y')$ and L_y denotes the extension of the material in the y direction. We observe that after translation of y and y', the $\bar{y}$ integral yields $2\pi\delta(k_y-k_y')$. Hence, we obtain

$$\frac{\langle|\hat{h}(k_x,k_z)|^2\rangle}{A_\parallel} = \left(\frac{\nu(1-2\nu)}{2\pi(1-\nu)\lambda}\right)^2 \frac{\int_{-\infty}^{\infty} \mathrm{d}k_y |\hat{g}(\underline{k})|^2 \frac{|\delta\hat{\lambda}(\underline{k})|^2}{V}}{|ik_x + \frac{2-3\nu}{2-\nu}|k_z||^2}, \tag{28}$$

where the brackets denote the average over $\bar{y}$ and $V = A_\parallel L_y$.

Our result Eq. (28) directly relates the two-dimensional power spectrum of height fluctuations in the fracture surface to the three-dimensional power spectrum of elastic modulus fluctuations. The former are frequently parametrised in terms of a roughness exponent ζ, such that the power spectrum scales with $k_\parallel = \sqrt{k_x^2 + k_z^2}$ as

$$\langle|\hat{h}(k_x,k_z)|^2\rangle \sim k_\parallel^{-2\zeta-2}, \tag{29}$$

where a broad range of measurements give $\zeta \approx 0.5$–0.8 (see for example Bouchaud, 1997). Whilst most of the cracks measured were dynamical and far from quasi-static, it is interesting to examine what inhomogeneity spectrum can lead to the same result from our quasi-static calculations. As $\hat{g}$ is homogeneous and of degree 0 in $\underline{k}$, one finds

$$|\delta\hat{\lambda}(\underline{k})|^2 \sim k^{-2\zeta-1} \tag{30}$$

is required, assuming the integral in Eq. (28) to converge as it does for $\zeta > 0$. Thus, within a quasi-static analysis, $\zeta \approx 0.8$ requires an inhomogeneity spectrum which is not compelling.

The function $\hat{g}(\underline{k})$ can be written as $|\hat{g}(\underline{k})|^2 = 4\pi^2 + \mathrm{order}(k_y^{-2})$ for large k_y. Thus, for $|\delta\hat{\lambda}(\underline{k})|^2$ falling off slower than k^{-1} (as, for example, for white noise), the integral in Eq. (28) diverges at large k_y. In particular, its leading order does not depend on k_x and k_z, yielding $\langle|\hat{h}(k_x,k_z)|^2\rangle \sim k_\parallel^{-2}$ and a roughness exponent of zero. This corresponds to the observations of Ball and Larralde on a brittle foam (see Larralde and Ball, 1995). This suggests that quasi-static fracture has a 'universal' roughness exponent of zero, and that the observations of Bouchaud correspond to a fundamentally different dynamical regime.

6. The real space disturbance of a crack near an inhomogeneity

In the last section on crack propagation near heterogeneities we shall investigate the disturbance of the crack in real space, i.e., $h(x,z)$. We assume that an initially planar crack propagates in an isotropic and otherwise homogeneous elastic material. The material has a point inhomogeneity at $\underline{a} = (a_x,a_y,a_z)$ with elastic constants $\lambda + \delta V \delta\lambda \delta(\underline{x}-\underline{a})$ and $\delta\mu = 0$, where λ and μ are the elastic constants of the bulk material. We recall that δV is the (infinitesimal) extension of the inclusion. We now want to investigate the real space height function for a point inhomogeneity. We may anticipate that the crack surface is disturbed in the vicinity of the inhomogeneity whereas it becomes flat further away. We obtain $\hat{h}(\ell_x,k_z)$ from the original evolution equation Eq. (21) to be

$$\begin{aligned} h_{k_z}(\ell_x) = {} & -\delta V \frac{\delta\lambda}{\lambda} \frac{\nu(1-2\nu)}{2\pi(1-\nu)} a_y |k_z|^3 \mathrm{e}^{-ik_z a_z} \mathrm{e}^{-|k_z|r} \int_{-\infty}^{\ell_x} \mathrm{d}x \mathrm{e}^{\frac{2-3\nu}{2-\nu}|k_z|(x-\ell_x)} \\ & \times \left(\frac{1}{(|k_z|r)^3} + \frac{2\nu}{2-\nu} \frac{1}{(|k_z|r)^2} + \frac{2|k_z|(a_x-x)}{(|k_z|r)^3} + \frac{2|k_z|(a_x-x)}{(|k_z|r)^4} \right), \end{aligned} \tag{31}$$

where $r = \sqrt{(a_x-x)^2 + a_y^2}$. Note that, as the crack is initially planar, $h_{k_z}(-\infty) = 0$. The integral in

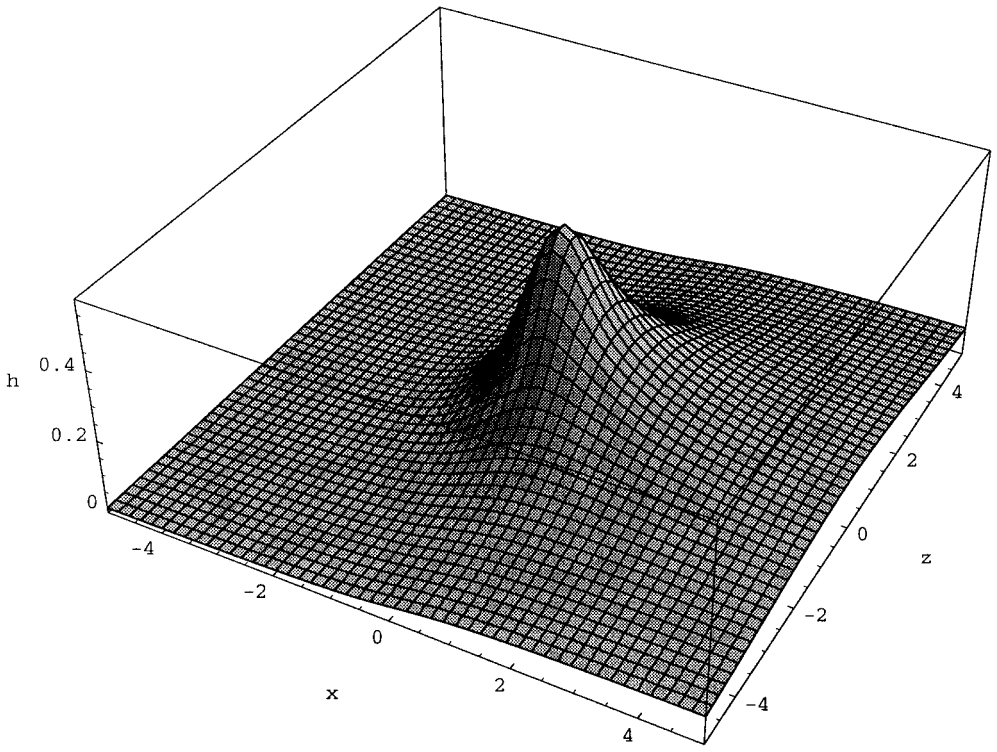

Fig. 2. The crack surface near a point inhomogeneity at $(0,a_y,0)$. The axes are normalised to a_y. Poisson's ratio is $\nu = 1/3$.

Eq. (31) can be written explicitly in terms of elementary functions. The explicit formula for $h(\ell_x,\ell_z)$ is derived in Appendix C. For the purpose of practical implementation, it is more convenient to start from the basic integral in Eq. (C6) and then to differentiate with respect to d, α_+ and α_-.

In Fig. 2, we see the evolution of the crack surface in the presence of a point inclusion at $(0,a_y,0)$ as a function the variables ℓ_x/a_y and z/a_y. The height function $h(\ell_x,z)$ is given by $h(\ell_x,z) = -\frac{\delta\lambda}{\lambda}\frac{\delta V}{4\pi^2 a_y^3}h$, where h is the dimensionless quantity in Fig. 2. Poisson's ratio is chosen to be $\nu = 1/3$. As anticipated, the distortion is maximal near the point inhomogeneity and flattens out further away. We also see that the perturbation decays slowly as the crack passes by the point inclusion.

In Fig. 3, we see line cuts of the crack surface along the ℓ_x-axis for different Poisson's ratios. We observe that $h(\ell_x,z,\underline{a})$ is not symmetric with respect to ℓ_x. The crack surface increases steeply near the inclusion and decreases comparatively slowly. A close examination shows that the maximum value of the height distortion is shifted towards positive ℓ_x. The shape of the crack surface near the inhomogeneity remains the same for all four Poisson's ratios; only the amplitude of the distortion increases modestly with larger ν. We may quantify these features by asymptotically expanding the rather complicated exact result.

It is often sufficient to know the asymptotic behaviour of $h(\ell_x,z,\underline{a})$ near and far away from the point inclusion. For ℓ_x/a_y, $z/a_y \ll 1$, we have

$$
\begin{aligned}
h(\ell_x,z,\underline{a}) \approx -\frac{\delta V}{a_y^2}\frac{\delta\lambda}{\lambda}\frac{\nu(2-\nu)(1-2\nu)}{2\pi^2(1-\nu)^2}\Bigg\{ & \frac{1+\gamma}{4\gamma^3\sqrt{1-\gamma^2}} \times \Bigg(\sqrt{1-\gamma^2}\big(-2\gamma-\gamma^3+\pi+\gamma^2\pi\big) \\
& + 2\big(-2-\gamma^2+\gamma^3\big)\arctan\left(\sqrt{\frac{1-\gamma}{1+\gamma}}\right)\Bigg) + \frac{3\left(\dfrac{\ell_x-a_x}{a_y}\right)^2}{8(-1+\gamma)\gamma^3} \\
& \Bigg(-8\gamma+4\gamma^3+\gamma^5+\gamma^4(1-2\pi)+4\pi-2\gamma^2\pi-\frac{2(8-8\gamma^2-3\gamma^4+\gamma^5)\arctan\left(\sqrt{\frac{1-\gamma}{1+\gamma}}\right)}{\sqrt{1-\gamma^2}}\Bigg) \\
& + \frac{\left(\dfrac{z-a_z}{a_y}\right)^2}{8(-1+\gamma)\gamma^5}\Bigg(24\gamma-8\gamma^3-9\gamma^5-3\gamma^6+2\gamma^7-12\pi+6\gamma^2\pi+6\gamma^4\pi \\
& + \frac{6(8-8\gamma^2-3\gamma^4+\gamma^5)\arctan\left(\sqrt{\frac{1-\gamma}{1+\gamma}}\right)}{\sqrt{1-\gamma^2}}\Bigg) \\
& + \frac{\dfrac{\ell_x-a_x}{a_y}\left(\gamma(6+3\gamma+5\gamma^2)+(6+6\gamma+4\gamma^2+4\gamma^3)\log\left(\dfrac{1}{1+\gamma}\right)\right)}{4\gamma^3}\Bigg\},
\end{aligned}
\tag{32}
$$

with $\gamma = \frac{2-3\nu}{2-\nu}$. In the special case where $\nu = 1/3$ (see Fig. 2), the above expression reduces to

$$
h(\ell_x,z,\underline{a}) \approx -\frac{\delta\lambda}{\lambda}\frac{\delta V}{4\pi^2 a_y^2}\left\{0.57317 + 0.15922\frac{\ell_x}{a_y} - 0.67754\frac{\ell_x^2}{a_y^2} - 0.46980\frac{z^2}{a_y^2}\right\}. \tag{33}
$$

The expansion far away from the inhomogeneity assumes only $\frac{\ell_x-a_x}{a_y} \gg 1$, i.e., z is left arbitrary. For positive $\frac{\ell_x-a_x}{a_y}$, as the crack passes by the inclusion, we obtain

$$
h(\ell_x,z,\underline{a}) \approx -\frac{\delta\lambda}{\lambda}\frac{\nu(2-\nu)(1-2\nu)}{2\pi^2(1-\nu)^2}\frac{\delta V}{a_y}\left\{\frac{2(1-\nu)(2-3\nu)(\ell_x-a_x)}{(2-3\nu)^2(\ell_x-a_x)^2+(2-\nu)^2(z-a_z)^2}\right\}. \tag{34}
$$

If $\delta\lambda(\underline{a})$ is a general distribution of inhomogeneities, the asymptotic value of $h(\ell_x,z)$ for $\ell_x \gg a_y$ is

$$
h(\ell_x,z) \approx -\int_\Omega \mathrm{d}^3 a \frac{\delta\lambda(\underline{a})}{\lambda}\frac{\nu(2-\nu)(1-2\nu)}{2\pi^2(1-\nu)^2}\frac{1}{a_y} \times \left\{\frac{2(1-\nu)(2-3\nu)(\ell_x-a_x)}{(2-3\nu)^2(\ell_x-a_x)^2+(2-\nu)^2(z-a_z)^2}\right\}. \tag{35}
$$

We can now imagine that we have a line of inhomogeneities parallel to the z-axis at a_y and $a_x = 0$, i.e.,

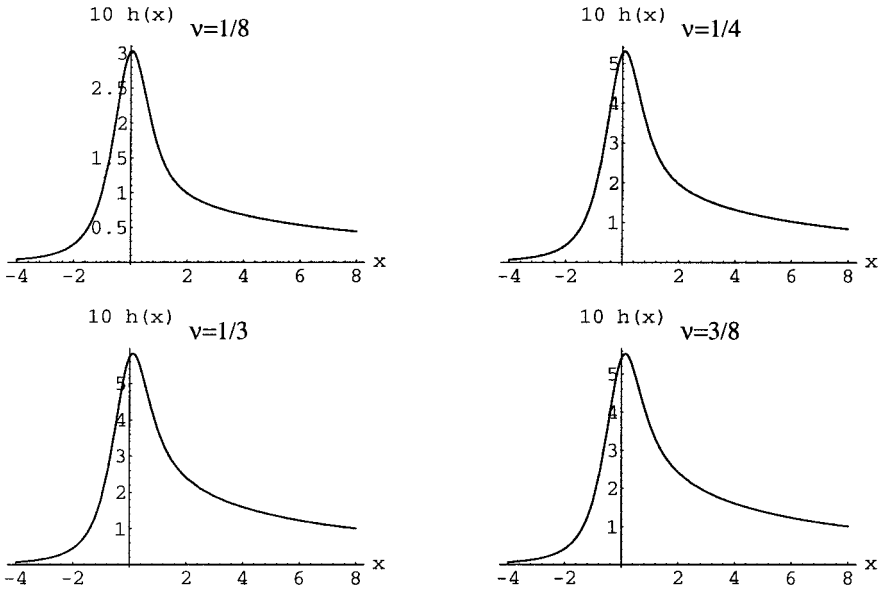

Fig. 3. Line plots of the crack surface $h(x,\ell_z=0)$ near a point inhomogeneity at $(0,a_y,0)$ for different values of Poisson's ratio. The crack surface is given by $h(x,\ell_z=0)=-\frac{\delta V}{4\pi a_y^2}h$, where h is the plotted quantity.

$\delta\lambda(\underline{x})=\delta A\delta\lambda\delta(x)\delta(y-a_y)$, where δA denotes the cross section of the line heterogeneity. Indeed, this is a two-dimensional model of a crack near an inhomogeneity. Then the integration in Eq. (35) yields

$$h(\ell_x,a_y)\approx -\frac{\delta\lambda}{\lambda}\frac{2\nu(1-2\nu)}{\pi(1-\nu)}\frac{\delta A}{a_y} \text{ for } \ell_x \gg a_y. \tag{36}$$

That means as the crack propagates it becomes planar again, but it is shifted by the amount given in Eq. (36).

We also observe that the crack is attracted towards an inhomogeneity if $\delta\lambda < 0$, and repulsed if $\delta\lambda > 0$, as shown here. This is in agreement with our physical understanding, since negative $\delta\lambda$ means that the inclusion is softer than the rest of the material. Hence, the strain around the inclusion is higher, and therefore, the crack is attracted towards the inclusion.

For a general distribution of inhomogeneities we obtain the height function by integrating $h(\ell_x,z,\underline{a})\delta\lambda(\underline{a})$ over the region occupied by the elastic material. All this suggests a great variety of interesting industrial applications, such as, 'guiding' a crack by the placing of appropriate inhomogeneities.

7. Conclusion

We have evaluated the path of a quasi-static crack near a heterogeneity with slightly different elastic constants from the bulk. We relate the Fourier transformed distribution of the heterogeneties to the power spectrum of the crack surface and thereby deduce a zero roughness exponent in quasi-

static crack propagation. This is in agreement with experimental observations by Larralde and Ball (1995). Bouchaud (1997) obtained a roughness exponent of 0.5–0.8 for dynamical cracks suggesting that the roughness exponent depends on the velocity of the crack. We strongly suggest further experimental investigation into the roughness of quasi-static crack surfaces. We also present closed analytic expressions for the crack surface in real space with asymptotic approximations close and far away from a point inhomogeneity.

Appendix A. The 3-D mode II weight function

The components of the mode II 3-D weight function for a planar semi-infinite crack are given by (see Al-Falou and Ball, 1998)

$$\mathscr{G}_{\mathrm{II},x}(x,y,k_z)=\sqrt{|k_z|}\Bigg[\big(8-12\nu+4\nu^2+(2-\nu)(\cos\phi+\cos 2\phi)+r|k_z|(-2+11\nu-8\nu^2+2\nu \cos\phi+(2-\nu)\cos 2\phi)\big)\frac{\sin\frac{\phi}{2}}{4(1-\nu)(2-\nu)}\frac{\mathrm{e}^{-r|k_z|}}{\sqrt{2\pi r|k_z|}}+\frac{1-2\nu}{2-\nu}\frac{|k_z|r\sin\phi}{2}\mathrm{e}^{r|k_z|\cos\phi} \operatorname{erfc}\left(\sqrt{2r|k_z|}\cos\frac{\phi}{2}\right)\Bigg], \tag{A1}$$

$$\mathscr{G}_{\mathrm{II},y}(x,y,k_z)=\sqrt{|k_z|}\Bigg[\big(4-10\nu+4\nu^2+(2-\nu)(\cos\phi-\cos 2\phi)+r|k_z|(-2+3\nu+4(1-\nu)\cos\phi -(2-\nu)\cos 2\phi)\big)\frac{\cos\left(\frac{\phi}{2}\right)}{4(1-\nu)(2-\nu)}\times\frac{\mathrm{e}^{-r|k_z|}}{\sqrt{2\pi r|k_z|}}-\frac{1-2\nu}{2(2-\nu)}\mathrm{e}^{r|k_z|\cos\phi}\operatorname{erfc}\left(\sqrt{2r|k_z|}\cos\frac{\phi}{2}\right)\Bigg] \tag{A2}$$

and

$$\mathscr{G}_{\mathrm{II},z}(x,y,k_z)=i\,\mathrm{sign}(k_z)\sqrt{|k_z|}\Bigg[\frac{\left(-1+\frac{5}{2}\nu-2\nu^2-\frac{2-\nu}{2}\cos\phi\right)\sin\frac{\phi}{2}}{(1-\nu)(2-\nu)}\times\sqrt{\frac{r|k_z|}{2\pi}}\mathrm{e}^{-r|k_z|} +\frac{1-2\nu}{2-\nu}\frac{r|k_z|\sin\phi}{2}\mathrm{e}^{r|k_z|\cos\phi}\operatorname{erfc}\left(\sqrt{2r|k_z|}\cos\frac{\phi}{2}\right)\Bigg], \tag{A3}$$

where $x=r\cos\phi$, $y=r\sin\phi$ and erfc denotes the complementary error function. The weight functions $\underline{\mathscr{G}}_{\mathrm{II},z}(x_0,y_0,k_z)$ as stated above, return the Fourier transformed mode II stress intensity factor $K_{\mathrm{II}}(k_z)$ for a volume force of the form $\underline{f}(\underline{x})=\underline{f}\delta(x-x_0)\delta(y-y_0)\mathrm{e}^{ik_z z}$. Fully in real space, $\underline{\mathscr{G}}_{\mathrm{II}}$ is given by

$$\underline{\mathscr{G}}_{\mathrm{II}}(Z,x,y,z) = \frac{1}{2\pi}\int_{-\infty}^{\infty} \mathrm{d}k_z \underline{\mathscr{G}}_{\mathrm{II}}(x,y,k_z)\mathrm{e}^{ik_z(z-Z)}. \tag{A4}$$

If $\underline{g}$ is an arbitrary loading applied at the crack surface and $\underline{f}$ a volume force, we obtain the mode II stress intensity factor at point Z along the crack tip in the form

$$K(Z) = \int_{\Omega} \mathrm{d}^3 x \underline{\mathscr{G}}_{\mathrm{II}}(Z,\underline{x}) \cdot \underline{f}(\underline{x}) + \int_{\partial\Omega} \mathrm{d}S \underline{\mathscr{G}}_{\mathrm{II}}(Z,\underline{x}(S)) \cdot \underline{g}(\underline{x}(S)), \tag{A5}$$

where Ω and $\partial\Omega$ are the domain and the boundary of the material, respectively.

Appendix B. The Fourier transformed Green function for a point inclusion

In this section, we want to Fourier transform the function $\hat{g}(x,y,k_z)$ in Eq. (23) with respect to x and y. We recall

$$\hat{g}(x,y,k_z) = -|k_z|^3 y \mathrm{e}^{-|k_z|r}\left(\frac{1}{(|k_z|r)^3} + \frac{2\nu}{2-\nu}\frac{1}{(|k_z|r)^2} - \frac{2|k_z|x}{(|k_z|r)^3} - \frac{2|k_z|x}{(|k_z|r)^4}\right), \tag{B1}$$

where $r = \sqrt{x^2+y^2}$. It is convenient to substitute x and y by the dimensionless variables $|k_z|x$ and $|k_z|y$ and to replace $k_x \to k_x/|k_z|$, $k_y \to k_y/|k_z|$. The Fourier integral is best decomposed into a regular part and a part which shall be regularised by differentiation. In the new variables the back Fourier transform reads

$$\begin{aligned}\hat{g}(k_x,k_y,k_z) = {} & \int_{-\pi}^{\pi}\mathrm{d}\phi\int_0^{\infty}\mathrm{d}r r\mathrm{e}^{-irk\cos(\phi-\psi)}\mathrm{e}^{-r}\left(\frac{2xy}{r^3} - \frac{2\nu}{2-\nu}\frac{y}{r^2}\right) + \int_{-\pi}^{\pi}\mathrm{d}\phi\int_0^{\infty}\mathrm{d}r r\mathrm{e}^{-irk\cos(\phi-\psi)} \\ & \mathrm{e}^{-r}\left(\frac{2xy}{r^4} - \frac{y}{r^3}\right),\end{aligned} \tag{B2}$$

where $x = r\cos\phi$, $y = r\sin\phi$, $k_x = k\cos\psi$ and $k_y = k\sin\psi$. The first integral in Eq. (B2) can be obtained by integrating with respect to r first and then to perform the angular integral by complex contour integration. In the second integral, we first differentiate with respect to k and then evaluate the integrals. Then the result needs to be integrated with respect to k. We obtain

$$\begin{aligned}\hat{g}(k_x,k_y,k_z) = {} & \frac{4\pi k_x k_y}{k^4}\left(2 - \frac{2+k^2}{\sqrt{1+k^2}}\right) + \frac{2\nu}{2-\nu}\frac{2\pi i k_y}{k^2}\left(1 - \frac{1}{\sqrt{1+k^2}}\right) \\ & + \frac{4\pi k_x k_y}{k^4}\left(\sqrt{1+k^2} - 1 - \frac{k^2}{2}\right) + \frac{2\pi i k_y}{k^2}(\sqrt{1+k^2} - 1).\end{aligned} \tag{B3}$$

Re-establishing the old variables and rearranging terms yields

$$\hat{g}(\underline{k}) = 2\pi \frac{k_x k_y k_z^2}{\left(k_x^2 + k_y^2\right)^2} \left(2 - \frac{k_x^2 + k_y^2}{k_z^2} - \frac{2|k_z|}{\sqrt{k_x^2 + k_y^2 + k_z^2}} \right) + 2\pi i k_y \times \left(\frac{1}{\sqrt{k_x^2 + k_y^2 + k_z^2}} - \frac{2 - 3\nu}{2 - \nu} \frac{k_z^2}{k_x^2 + k_y^2} \left(\frac{1}{|k_z|} - \frac{1}{\sqrt{k_x^2 + k_y^2 + k_z^2}} \right) \right). \tag{B4}$$

Appendix C. Evaluation of the real space crack surface

We assume that an initially planar crack propagates in an isotropic and otherwise homogeneous elastic material. The material has a point inhomogeneity at $\underline{a} = (0, a_y, 0)$ with elastic constants $\lambda + \delta V \delta\lambda \delta(\underline{x} - \underline{a})$ and $\delta\mu = 0$. λ and μ are the elastic constants of the material. We obtain $h(\ell_x, k_z)$ from the original evolution equation Eq. (21) to be

$$h_{k_z}(\ell_x) = -\delta V \frac{\delta\lambda}{\lambda} \frac{\nu(1-2\nu)}{2\pi(1-\nu)} a_y |k_z|^3 \mathrm{e}^{-ik_z a_z} \mathrm{e}^{-|k_z| r} \int_{-\infty}^{\ell_x} \mathrm{d}x \mathrm{e}^{\frac{2-3\nu}{2-\nu}|k_z|(x-\ell_x)} \times \left(\frac{1}{(|k_z| r)^3} + \frac{2\nu}{2-\nu} \frac{1}{(|k_z| r)^2} + \frac{2|k_z|(a_x - x)}{(|k_z| r)^3} + \frac{2|k_z|(a_x - x)}{(|k_z| r)^4} \right), \tag{C1}$$

where $r = \sqrt{(a_x - x)^2 + a_y^2}$. Note that $h_{k_z}(-\infty) = 0$ as the crack is initially planar. The substitution $u = \frac{a_x - x}{a_y}$ further simplifies Eq. (C1) to

$$h_{k_z}(\ell_x) = -\frac{\delta\lambda}{\lambda} \frac{\nu(1-2\nu)}{2\pi(1-\nu)} \frac{\delta V}{a_y} \int_{\frac{a_x - \ell_x}{a_y}}^{\infty} \mathrm{d}x \mathrm{e}^{-|k_z| a_y \left(\frac{2-3\nu}{2-\nu} \left(x - \frac{a_x - \ell_x}{a_y} \right) + r \right)} \mathrm{e}^{-ik_z a_z} \left(\frac{1}{r^3} + \frac{2x}{r^4} + \frac{2\nu}{2-\nu} \frac{|k_z| a_y}{r^2} + \frac{2|k_z| a_y x}{r^3} \right), \tag{C2}$$

where $r = \sqrt{x^2 + 1}$. It is more convenient to first perform the back Fourier transform with respect to k_z

$$h(\ell_x, z) = -\frac{\delta\lambda}{\lambda} \frac{\nu(1-2\nu)}{4\pi^2(1-\nu)} \frac{\delta V}{a_y} \int_{\frac{a_x - \ell_x}{a_y}}^{\infty} \mathrm{d}x \int_0^{\infty} \mathrm{d}k_z \mathrm{e}^{-k_z a_y \left(\frac{2-3\nu}{2-\nu} \left(x - \frac{a_x - \ell_x}{a_y} \right) + r + i \frac{a_z - z}{a_y} \right)} \times \left(\frac{1}{r^3} + \frac{2x}{r^4} + \frac{2\nu}{2-\nu} \frac{k_z a_y}{r^2} + \frac{2 k_z a_y x}{r^3} \right) + c.c. \tag{C3}$$

$$h(\ell_x,z) = -\frac{\delta\lambda}{\lambda}\frac{\nu(1-2\nu)}{4\pi^2(1-\nu)}\frac{1}{a_y^2}\int_{\frac{a_x-\ell_x}{a_y}}^{\infty} \mathrm{d}x \left\{ \frac{\frac{1}{r^3}+\frac{2x}{r^4}}{\frac{2-3\nu}{2-\nu}x + r - \frac{2-3\nu}{2-\nu}\frac{a_x-\ell_x}{a_y} + i\frac{a_z-z}{a_y}} \right.$$

$$\left. + \frac{\frac{2\nu}{2-\nu}\frac{1}{r^2}+\frac{2x}{r^3}}{\left(\frac{2-3\nu}{2-\nu}x + r - \frac{2-3\nu}{2-\nu}\frac{a_x-\ell_x}{a_y} + i\frac{a_z-z}{a_y}\right)^2} \right\} + c.c. \tag{C4}$$

In the last integral, we first substitute $x = \sinh u$ followed by the substitution $t = \mathrm{e}^u$ to obtain

$$h(\ell_x,z) = -\frac{\delta\lambda}{\lambda}\frac{2\nu(1-2\nu)}{\pi^2(1-\nu)}\frac{\delta V}{a_y^2}\int_{\frac{a_x-\ell_x}{a_y}+\sqrt{1+\left(\frac{a_x-\ell_x}{a_y}\right)^2}}^{\infty} \mathrm{d}t$$

$$\left\{ \frac{t^2}{(1+t^2)^3}\frac{3t^2-1}{\left(\frac{2-3\nu}{2-\nu}+1\right)t^2 - 2\left(\frac{2-3\nu}{2-\nu}\frac{a_x-\ell_x}{a_y} - i\frac{a_z-z}{a_y}\right)t + \left(1-\frac{2-3\nu}{2-\nu}\right)} + \frac{t^2}{(1+t^2)^2} \right.$$

$$\left. \times \frac{\left(\frac{2\nu}{2-\nu}+2\right)t^2 + \left(\frac{2\nu}{2-\nu}-2\right)}{\left[\left(\frac{2-3\nu}{2-\nu}+1\right)t^2 - 2\left(\frac{2-3\nu}{2-\nu}\frac{a_x-\ell_x}{a_y} - i\frac{a_z-z}{a_y}\right)t + \left(1-\frac{2-3\nu}{2-\nu}\right)\right]^2} \right\} + c.c. \tag{C5}$$

This is a standard integral of a rational function which can be derived (through differentiation with respect to d, α_+ and α_-) from the integral

$$\int_a^{\infty} \mathrm{d}x \frac{1}{x^2+d^2}\frac{1}{(x-\alpha_+)(x-\alpha_-)}$$

$$= \frac{\log(a+id)}{2id\left(\alpha_+\alpha_- + id(\alpha_+ + \alpha_-) - d^2\right)} - \frac{\log(a-id)}{2id\left(\alpha_+\alpha_- - id(\alpha_+ + \alpha_-) - d^2\right)} - \frac{\log(a-\alpha_+)}{(\alpha_+ - \alpha_-)\left(\alpha_+^2 + d^2\right)}$$

$$+ \frac{\log(a-\alpha_-)}{(\alpha_+ - \alpha_-)\left(\alpha_-^2 + d^2\right)}, \tag{C6}$$

where

$$\alpha_{\pm} = \frac{2-\nu}{4(1-\nu)}\left[\frac{2-3\nu}{2-\nu}\frac{a_x-\ell_x}{a_y} + i\frac{z-a_z}{a_y} \pm \sqrt{\left(\frac{2-3\nu}{2-\nu}\frac{a_x-\ell_x}{a_y} + i\frac{z-a_z}{a_y}\right)^2 + \left(\frac{2-3\nu}{2-\nu}\right)^2 - 1}\right] \tag{C7}$$

and

$$a = \frac{a_x - \ell_x}{a_y} + \sqrt{1 + \left(\frac{a_x - \ell_x}{a_y}\right)^2}. \tag{C8}$$

References

Al-Falou, A.A., Ball, R.C., 1999. The 3-D weight function for a quasi-static planar crack. Int. J. Solids Structures (in press).
Al-Falou, A.A., Larralde, H., Ball, R.C., 1998. Effect of T-stresses on the path of a three-dimensional crack propagating quasistatically under type I loading. Int. J. Solids Structures 34 (5), 569.
Ball, R.C., Larralde, H., 1995. Linear stability analysis of planar straight cracks propagating quasistatically under type I loading. Int. J. Fract. 71, 365.
Bouchaud, E., 1997. Scaling properties of cracks. J. Phys., Condensed Matter 9, 4319.
Freund, L.B., 1993. Dynamic Fracture Mechanics. Cambridge University Press.
Gao, H., 1992. Three-dimensional slightly nonplanar cracks. J. Appl. Mech. 59, 335.
Larralde, H., Ball, R.C., 1995. The shape of slowly growing cracks. Europhys. Lett. 30 (2), 87.
Lawn, B., 1993. Fracture of Brittle Solids. Cambridge University Press.
Sih, G.C., 1973. In: Handbook of Stress Intensity Factors, Lehigh University, Bethlehem Pennsylvania, p.3.2.7–1.
Xu, G., Bower, A.F., Oritz, M., 1994. An analysis of non-planar crack growth under mixed mode loading. Int. J. Solids Structures 31 (16), 2167.